

AccFFT: A library for distributed-memory FFT on CPU and GPU architectures

Amir Gholami^{a,*}, Judith Hill^b, Dhairyा Malhotra^a, George Biros^a

^a*Institute for Computational Engineering and Sciences,*

The University of Texas at Austin, Austin, TX 78712, USA

^b*Computer Science and Mathematics Division,*

Oak Ridge National Laboratory, Oak Ridge, TN 37831, USA

Abstract

We present a new library for parallel distributed Fast Fourier Transforms (FFT). Despite the large amount of work on FFTs, we show that significant speedups can be achieved for distributed transforms. The importance of FFT in science and engineering and the advances in high performance computing necessitate further improvements. AccFFT extends existing FFT libraries for x86 architectures (CPUs) and CUDA-enabled Graphics Processing Units (GPUs) to distributed memory clusters using the Message Passing Interface (MPI). Our library uses specifically optimized all-to-all communication algorithms, to efficiently perform the communication phase of the distributed FFT algorithm. The GPU based algorithm, effectively hides the overhead of PCIe transfers. We present numerical results on the Maverick and Stampede platforms at the Texas Advanced Computing Center (TACC) and on the Titan system at the Oak Ridge National Laboratory (ORNL). We compare the CPU version of AccFFT with P3DFFT and PFFT libraries and we show a consistent $2 - 3 \times$ speedup across a range of processor counts and problem sizes. The comparison of the GPU code with FFTE library shows a similar trend with a $2 \times$ speedup. The library is tested up to 131K cores and 4,096 GPUs of Titan, and up to 16K cores of Stampede.

Keywords: Fast Fourier Transform, Parallel FFT, Distributed FFT, slab decomposition, pencil decomposition

1. Introduction

Fast Fourier Transform is one of the most fundamental algorithms in computational science and engineering. It is used in turbulence simulations [20], computational chemistry and biology [9], gravitational interactions [3], cardiac electro-physiology [7], cardiac mechanics [22], acoustic, seismic and electromagnetic scattering [6, 30], materials science [23], molecular docking [19] and many other areas.

Due to its wide range of applications and the need for scalability and performance, the design of FFT al-

gorithms remains an active area of research. Highly optimized single-node FFT algorithms have been implemented by all major hardware vendors, including Intel’s MKL library [40], IBM’s ESSL library [11], NVIDIA’s CUFFT [26] library, and the new AMD’s clFFT library [1]. In the realm of open-source software, one of the most widely used libraries is the FFTW [14, 13]. Single-node implementations of these libraries have been extended to distributed memory versions either by the original developers or by other research groups and a large number of distributed memory libraries is currently available.

Then, what’s the reason to design yet another library on FFTs? Despite the significant amount of work that has taken place on optimizing single node FFT computa-

*Corresponding author

Email addresses: gholami@accfft.org (Amir Gholami),
hilljc@ornl.gov (Judith Hill), dhairyamalhotra@gmail.com (Dhairyा Malhotra), gbiros@acm.org (George Biros)

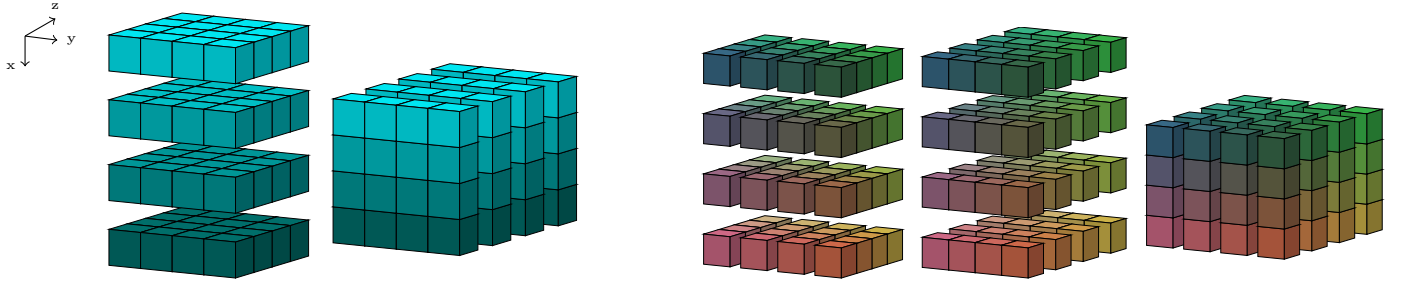


Figure 1: Decomposition of the input/output array in different stages of the forward FFT algorithm. Left: slab decomposition. Right: pencil decomposition

tions, there is still a gap for an efficient distributed library. Many applications require strong scaling because the time-to-solution needs to be as small as possible. Typically FFT calls are invoked thousands of times within an application, for example, as part of time-stepping or Monte Carlo sampling. Often the FFT is the slowest part of the computation due to the communication costs. Therefore, small relative speedups in the FFT can result in significant absolute wall-clock gains. Second, hybrid parallelism support is not as extensive as plain MPI—especially regarding integration of MPI-based parallelism combined with accelerators. Third, the performance of the FFT can vary significantly depending on the problem size, the underlying network, and the number of processors used. Fourth, some applications require scaling to million of cores, in which case the communication costs significantly limit scalability. In a nutshell, FFT libraries need to deliver scalability from a single MPI rank to 100s of thousands of MPI ranks, while using all available system resources. This poses significant challenges to the design and implementation of an efficient library.

Contributions. We present AccFFT, a library that given an $N_0 \times N_1 \times N_2 \times \dots$ matrix of values computes its Fourier Transform. The library supports the following features:

- hybrid MPI and OpenMP parallelism,
- hybrid MPI and CUDA parallelism,
- specifically optimized all-to-all exchange algorithms

for both CPU and GPU

- slab (or 1D) and pencil (or 2D) decomposition,
- and real-to-complex (R2C) and complex-to-complex (C2C) transforms.

AccFFT uses CUFFT and FFTW for the FFT computations. AccFFT extends the single-node version of these two libraries to pencil decomposition for distributed memory FFTs. Both decompositions are necessary in order to ensure good performance across a range of MPI ranks. Slab decomposition limits the number of MPI ranks, P , to be less or equal to $N_0 = \max\{N_0, N_1, N_2\}$, and thus is not as scalable as the pencil decomposition. Typical values for N range from 100s to 10,000s. When the FFT size is large, the all-to-all phase of the algorithm adversely affects the scaling and becomes the major bottleneck. Our custom all-to-all scheme significantly improves the performance of AccFFT. The optimal configuration for a given problem size and processor count is determined automatically using a planning or setup phase.

We compare our code experimentally with P3DFFT [29] and PFFT [31] on three different HPC platforms. We perform strong scaling on Maverick (with K40 GPUs) and Stampede (with Intel Xeon) at TACC, and Titan at ORNL (with K20 GPUs). Overall, our implementation improves the scaling, and gets a consistent speedup of $2 - 3 \times$ across a range of test configurations. We use novel communication algorithms for GPUs to hide the overhead of moving data forth and back from the CPU. Even though we do

Algorithm 1: Forward and backward FFT algorithm for slab decomposition.

Input : Data in spatial domain.

Layout: $N_0/P \times N_1 \times N_2$

Output: Data in frequency domain.

Layout: $\widehat{N}_0 \times \widehat{N}_1 / P \times \widehat{N}_2$

$$N_0/P \times \widehat{N}_1 \times \widehat{N}_2 \xleftarrow{FFT} N_0/P \times N_1 \times N_2; \\ N_0 \times \widehat{N}_1 / P \times \widehat{N}_2 \xleftarrow{T} N_0/P \times \widehat{N}_1 \times \widehat{N}_2; \\ \widehat{N}_0 \times \widehat{N}_1 / P \times \widehat{N}_2 \xleftarrow{FFT} N_0 \times \widehat{N}_1 / P \times \widehat{N}_2;$$

Input : Data in frequency domain.

Layout: $\widehat{N}_0 \times \widehat{N}_1 / P_0 \times \widehat{N}_2$

Output: Data in spatial domain.

Layout: $N_0/P_0 \times N_1 \times N_2$

$$N_0 \times \widehat{N}_1 / P_0 \times \widehat{N}_2 \xleftarrow{IFFT} \widehat{N}_0 \times \widehat{N}_1 / P_0 \times \widehat{N}_2; \\ N_0/P_0 \times \widehat{N}_1 \times \widehat{N}_2 \xleftarrow{T} N_0 \times \widehat{N}_1 / P_0 \times \widehat{N}_2; \\ N_0/P_0 \times N_1 \times N_2 \xleftarrow{IFFT} N_0/P_0 \times \widehat{N}_1 \times \widehat{N}_2;$$

not use GPUDirect technology, the GPU results are either better or almost the same as the CPU times. Comparison of the GPU code with FFTE [36] library shows a consistent speedup of $2\times$. The library is open source and available for download [2].

Related work. There is a vast literature on algorithms for FFTs. Our discussion is by no-means exhaustive. We limit it on the work that is most closely related to ours. Introductory material on distributed memory FFT can be found in [16]. Excellent discussions on complexity and performance analysis for 3-D FFTs can be found in [15] and [8].

- (*Libraries for CPU architectures.*) One of the most widely used packages for FFTs is the FFTW [14] library. FFTW supports MPI using slab decomposition and hybrid parallelism using OpenMP. As mentioned above, the scalability of slab decompositions is limited. Furthermore, FFTW does not support GPUs. P3DFFT [29] extends the single-node FFTW (or ESSL) and supports both slab and pencil decompositions. P3DFFT does not use any special scheme for performing the all-to-all communication, and currently does not support hybrid parallelism¹. P3DFFT is a well written library that has been used extensively. Another recent library is PFFT [31]. The library is built on top of FFTW and uses its transpose functions to perform the communication phase. It has recently been extended to nonequispaced FFTs [32]. Neither of the libraries, use any special algorithm to optimize

communication phase or can be used with GPUs. A very similar code to P3DFFT and PFFT is 2DECOMP [21] and OpenFFT [10].

A multithreaded code (not open source) is described in [20] in the context of turbulence simulations. This code is based on FFTW and employs single-node optimizations. To our knowledge, this code is one of the most scalable 3-D FFTs. The authors report results on up 786,432 cores on an IBM Blue Gene machine. However, the authors observe lack of scalability of the transpose for large core counts. On Stampede they start loosing scalability at 4,098 nodes. In [34] the authors propose pencil decomposition optimizations that deliver $1.8\times$ speed-up over FFTW. The main idea is the use of non-blocking MPI all-to-all operations that allow overlapping computation and communication. However the method does not address the scalability issues of FFTs. The authors compare FFTW, P3DFFT and 2DECOMP with their scheme. Other works that study 3-D FFTs on x86 platforms include [4, 27].

- (*Libraries for distributed-memory GPUs.*) The work presented in [25] is, to our knowledge, one the most efficient and more scalable distributed GPU implementations. It only supports slab decomposition so it cannot be scaled to large core counts. The scaling results presented in the paper are up to 768 GPUs. The authors employ special techniques to improve the complexity of the transpose and use an in-house CUDA FFT implementation. Their optimizations are specific to the infiniband-interconnect using the IBverbs library and thus is not portable. In the largest run, they observed 4.8TFLOPS for a 2048^3 problem

¹The support for hybrid parallelism is on the to do list of P3DFFT and may be added in the future.

Algorithm 2: Forward and backward FFT algorithm for pencil decomposition.

Input : Data in spatial domain.

Layout: $N_0/P_0 \times N_1/P_1 \times N_2$

Output: Data in frequency domain.

Layout: $\widehat{N}_0 \times \widehat{N}_1/P_0 \times \widehat{N}_2/P_1$

$$\begin{aligned} N_0/P_0 \times N_1/P_1 \times \widehat{N}_2 &\xleftarrow{\text{FFT}} N_0/P_0 \times N_1/P_1 \times N_2; \\ N_0/P_0 \times N_1 \times \widehat{N}_2/P_1 &\xleftarrow{T} N_0/P_0 \times N_1/P_1 \times \widehat{N}_2; \\ N_0/P_0 \times \widehat{N}_1 \times \widehat{N}_2/P_1 &\xleftarrow{\text{FFT}} N_0/P_0 \times N_1 \times \widehat{N}_2/P_1; \\ N_0 \times \widehat{N}_1/P_0 \times \widehat{N}_2/P_1 &\xleftarrow{T} N_0/P_0 \times \widehat{N}_1 \times \widehat{N}_2/P_1; \\ \widehat{N}_0 \times \widehat{N}_1/P_0 \times \widehat{N}_2/P_1 &\xleftarrow{\text{FFT}} N_0 \times \widehat{N}_1/P_0 \times \widehat{N}_2/P_1; \end{aligned}$$

Input : Data in frequency domain.

Layout: $\widehat{N}_0 \times \widehat{N}_1/P_0 \times \widehat{N}_2/P_1$

Output: Data in spatial domain.

Layout: $N_0/P_0 \times N_1/P_1 \times N_2$

$$\begin{aligned} N_0 \times \widehat{N}_1/P_0 \times \widehat{N}_2/P_1 &\xleftarrow{\text{IFFT}} \widehat{N}_0 \times \widehat{N}_1/P_0 \times \widehat{N}_2/P_1; \\ N_0/P_0 \times \widehat{N}_1 \times \widehat{N}_2/P_1 &\xleftarrow{T} N_0 \times \widehat{N}_1/P_0 \times \widehat{N}_2/P_1; \\ N_0/P_0 \times N_1 \times \widehat{N}_2/P_1 &\xleftarrow{\text{IFFT}} N_0/P_0 \times \widehat{N}_1 \times \widehat{N}_2/P_1; \\ N_0/P_0 \times N_1/P_1 \times \widehat{N}_2 &\xleftarrow{T} N_0/P_0 \times N_1 \times \widehat{N}_2/P_1; \\ N_0/P_0 \times N_1/P_1 \times N_2 &\xleftarrow{\text{IFFT}} N_0/P_0 \times N_1/P_1 \times \widehat{N}_2; \end{aligned}$$

on 786 M2050 Fermi GPUs (double precision, complex-to-complex), which is roughly 1.2% of the peak performance.

The DiGPUFFT open source library [8] is a modification of P3DFFT in which the intranode computations are replaced by CUFFT but no further optimization were performed and as a result they get about 0.7% of the peak. However, DiGPUFFT code was not designed for production but for experimental validation of the theoretical analysis of the complexity of 3-D FFTs, and its implications to the design of exascale architectures.

- *(1D FFT and single-node libraries.)* Other works that analyze scalability of the FFT codes include the FFTE code [37] (which is part of the HPCC benchmark) that includes several optimizations but has support for GPU only with PGI compiler directives. In [41, 17] the authors propose schemes for single node 3-D FFTs. In [24], shared-memory multiple GPU algorithms are discussed. More specialized and somewhat machine-dependent codes are [18] and [12].

A very interesting set of papers proposes a different FFT algorithm that has lower global communication constants (it requires one as opposed to three all-to-all communications) and can be made even faster (up to 2 \times) by introducing an approximation error in the numerical calculations. The algorithm was introduced in [38] and its parallel implementation discussed in [28]. Now it is part of the MKL library. It currently supports 1D FFT transforms only.

Limitations. There are several limitations in our library. Currently we do not support pruned FFTs or additional features such as Chebyshev approximations. The library only supports double precision FFTs, although the work on single precision version is on going. Our implementation does not support inexact FFTs. Currently there is no support for hybrid floating point computation, but for larger FFTs it may be necessary.

Outline of the paper. In the next section we discuss the distributed FFT algorithm. In Section 2, we summarize our algorithms for CPU and GPU platforms, and discuss details of our optimizations. In Section 3, we present results of the numerical experiments.

2. Algorithm

In this section we discuss the AccFFT library's algorithms. First let us introduce some basic notation: f is input array, \widehat{f} is its Fourier transform, P is the total number of MPI tasks, N_0, N_1, N_2 denotes the size of f in x,y, and z direction, and $N = N_0 \times N_1 \times N_2$.

The discrete 3-D Fourier transform corresponds to a dense matrix-vector multiplication. However, the computational complexity can be reduced by using Cooley-Turkey algorithm to:

$$5N_0N_1N_2(\log(N_0N_1N_2)).$$

The forward FFT maps space to frequency domain and the inverse FFT maps the frequency to space domain. The

Algorithm 3: Forward and backward FFT algorithms for general d dimensional decomposition.

Input : Data in spatial domain.

Layout: $N_0/P_0 \times \cdots \times N_d$

Output: Data in frequency domain.

Layout: $\widehat{N}_0 \times \cdots \times \widehat{N}_d/P_{d-1}$

$h = N_0/P_0 \times \cdots \times N_{d-1}/P_{d-1};$

$h' = 1;$

for $i \in d, \dots, 1$ **do**

| |
|---|
| $h \times \widehat{N}_i \times h' \xleftarrow{\text{FFT}} h \times N_i \times h';$ |
| $H = h/(\widehat{N}_{i-1}/P_{i-1});$ |
| $H' = h' * (\widehat{N}_i/P_{i-1});$ |
| $H \times \widehat{N}_{i-1} \times H' \xleftarrow{T} h \times \widehat{N}_i \times h';$ |
| $h = H; h' = H';$ |

Input : Data in frequency domain.

Layout: $\widehat{N}_0 \times \cdots \times \widehat{N}_d/P_{d-1}$

Output: Data in spatial domain.

Layout: $N_0/P_0 \times \cdots \times N_d$

$h = 1;$

$h' = \widehat{N}_1/P_0 \times \cdots \times \widehat{N}_d/P_{d-1};$

for $i \in 0, \dots, d$ **do**

| |
|---|
| $h \times N_i \times h' \xleftarrow{\text{IFFT}} h \times \widehat{N}_i \times h';$ |
| $H = h * (N_i/P_i);$ |
| $H' = h' / (\widehat{N}_{i+1}/P_i);$ |
| $H \times \widehat{N}_{i+1} \times H' \xleftarrow{T} h \times \widehat{N}_i \times h';$ |
| $h = H; h' = H';$ |

algorithms are the same up to a scaling factor, and have the same computational complexity.

For many scientific applications, f does not fit into a single node and therefore the data needs to be distributed across several nodes. Two such distributions for a 3D array are the slab decomposition, in which the data is distributed in slabs and the pencil decomposition where each task gets a pencil of the data, as shown in Figure 1. To compute the FFT, each task has to compute its portion of FFTs, and then exchange data with other tasks. One can either use a binary exchange or a transpose (all-to-all) algorithm [16]. In this paper we focus on the latter.

First we discuss the slab-decomposition, which is outlined in Algorithm 1. The input data is distributed in the first dimension over P tasks, i.e. $N_0/P \times N_1 \times N_2$, which is referred as a slab. Without loss of generality let us assume that $N_0 = \max\{N_0, N_1, N_2\}$. In the limit of $P = N_0$, each task will just get a 2D slice of f locally. If $P > N_0$ the slab decomposition cannot be used. In the forward algorithm, each task computes a N_0/P -batch of 2-D FFTs, each one having a size of $N_1 \times N_2$. Then an all-to-all exchange takes place to redistribute the data (indicated by the second step marked as T in Algorithm 1). After this each task gets a slab of size $N_0 \times \widehat{N}_1/P \times \widehat{N}_2$, where the hats denote that the Fourier Transform has been computed across the last two dimensions. To complete the transform, each task can

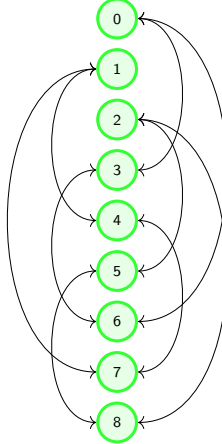
then compute a $\widehat{N}_1/P \times \widehat{N}_2$ -batch of 1-D FFTs of length N_0 . The inverse FFT can be computed in a similar fashion by reversing these steps. One advantage of our implementation is that the memory layout of the data in frequency space is the same as in the spatial one. This is different than FFTW’s implementation where the default (and faster) option, changes the memory layout from xyz to yxz².

Slab decomposition can be modified by decomposing the second dimension as well, which is known as pencil decomposition (Algorithm 2). In this approach each task gets a batch of 1-D pencils, local in the last dimension. That is the memory layout of the data in each task is $N_0/P_0 \times N_1/P_1 \times N_2$. The MPI tasks are mapped to a 2D matrix with P_0 rows and P_1 columns such that $P = P_0 \times P_1$. To compute the forward FFT, each task first computes a $N_0/P_0 \times N_1/P_1$ batch of 1-D FFTs of length N_2 . This is followed by a block row-wise all-to-all communication step in which all the tasks in the same row call exchange to collect the second dimension of the array locally. In this step, one needs to redistribute a batch of N_0/P_0 matrices of size $N_1/P_1 \times N_2$. A naive implementation of this phase would lead to costly cache misses. As a result, we first perform a local packing of the data, so

²FFTW3 provides an option which brings back the memory to its original format at the cost of a local transpose.

| | | | | | | | | |
|----|----|----|----|----|----|----|----|----|
| 0 | 1 | 2 | 3 | 4 | 5 | 6 | 7 | 8 |
| 9 | 10 | 11 | 12 | 13 | 14 | 15 | 16 | 17 |
| 18 | 19 | 20 | 21 | 22 | 23 | 24 | 25 | 26 |
| 27 | 28 | 29 | 30 | 31 | 32 | 33 | 34 | 35 |
| 36 | 37 | 38 | 39 | 40 | 41 | 42 | 43 | 44 |
| 45 | 46 | 47 | 48 | 49 | 50 | 51 | 52 | 53 |
| 54 | 55 | 56 | 57 | 58 | 59 | 60 | 61 | 62 |
| 63 | 64 | 65 | 66 | 67 | 68 | 69 | 70 | 71 |
| 72 | 73 | 74 | 75 | 76 | 77 | 78 | 79 | 80 |

(a)

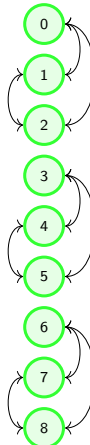


| | | | | | | | | |
|----|----|----|----|----|----|----|----|----|
| 0 | 1 | 2 | 27 | 28 | 29 | 54 | 55 | 56 |
| 9 | 10 | 11 | 36 | 37 | 38 | 63 | 64 | 65 |
| 18 | 19 | 20 | 45 | 46 | 47 | 72 | 73 | 74 |
| 3 | 4 | 5 | 30 | 31 | 32 | 57 | 58 | 59 |
| 12 | 13 | 14 | 39 | 40 | 41 | 66 | 67 | 68 |
| 21 | 22 | 23 | 48 | 49 | 50 | 75 | 76 | 77 |
| 6 | 7 | 8 | 33 | 34 | 35 | 60 | 61 | 62 |
| 15 | 16 | 17 | 42 | 43 | 44 | 69 | 70 | 71 |
| 24 | 25 | 26 | 51 | 52 | 53 | 78 | 79 | 80 |

(b)

| | | | | | | | | |
|----|----|----|----|----|----|----|----|----|
| 0 | 27 | 54 | 1 | 28 | 55 | 2 | 29 | 56 |
| 9 | 36 | 63 | 10 | 37 | 64 | 11 | 38 | 65 |
| 18 | 45 | 72 | 19 | 46 | 73 | 20 | 47 | 74 |
| 3 | 30 | 57 | 4 | 31 | 58 | 5 | 32 | 59 |
| 12 | 39 | 66 | 13 | 40 | 67 | 14 | 41 | 68 |
| 21 | 48 | 75 | 22 | 49 | 76 | 23 | 50 | 77 |
| 6 | 33 | 60 | 7 | 34 | 61 | 8 | 35 | 62 |
| 15 | 42 | 69 | 16 | 43 | 70 | 17 | 44 | 71 |
| 24 | 51 | 78 | 25 | 52 | 79 | 26 | 53 | 80 |

(c)



| | | | | | | | | |
|---|----|----|----|----|----|----|----|----|
| 0 | 9 | 18 | 27 | 36 | 45 | 54 | 63 | 72 |
| 1 | 10 | 19 | 28 | 37 | 46 | 55 | 64 | 73 |
| 2 | 11 | 20 | 29 | 38 | 47 | 56 | 65 | 74 |
| 3 | 12 | 21 | 30 | 39 | 48 | 57 | 66 | 75 |
| 4 | 13 | 22 | 31 | 40 | 49 | 58 | 67 | 76 |
| 5 | 14 | 23 | 32 | 41 | 50 | 59 | 68 | 77 |
| 6 | 15 | 24 | 33 | 42 | 51 | 60 | 69 | 78 |
| 7 | 16 | 25 | 34 | 43 | 52 | 61 | 70 | 79 |
| 8 | 17 | 26 | 35 | 44 | 53 | 62 | 71 | 80 |

(d)

Figure 2: Demonstration of the kway all-to-all for $k = 3$. Each element of the matrix represents a contiguous super-element in memory. Memory addresses increase from left to right and top to bottom (C style). The input matrix is shown in (a), which is distributed to $P = 9$ processes. In the first stage, each process sends/receives data to/from $k - 1$ processes. The received data after this communication (b), is reshuffled to make the data contiguous for the next communication stage (c). A final all-to-all and reshuffling results in the global transpose (d). The kway all-to-all is expected to finish in $2 = \log_3 9$ stages as shown. Point-to-point all-to-all would have completed in one stage by posting all send/receives in one step.

that all the batched noncontiguous data, are grouped together in a contiguous buffer. Then the all-to-all operation is performed, followed by an unpacking operation to get the data back into its correct format. Another approach is to use MPI data types to exchange non contiguous data. However, we found the latter to have an inferior performance.

After the first all-to-all exchange, each task computes a batched 1-D FFT of size N_1 of its local data, which is now in the form of $N_0/P_0 \times N_1 \times \widehat{N}_2/P_1$. This is followed by a

column-wise all-to-all exchange. In this step, the all-to-all operation is performed on a $N_0/P_0 \times N_1$ matrix with super-elements of size \widehat{N}_2/P_1 complex numbers. In this step, the data is indeed contiguous and no packing/unpacking is required. However, we do perform a local transpose, to change the memory layout from $N_1/P_0 \times N_0 \times N_2/P_1$ to $N_0 \times N_1/P_0 \times N_2/P_1$. This is done to have a consistent memory access pattern in both the spatial and frequency domain, which is desirable from a user's standpoint. To complete the forward FFT, a final batched 1-D FFT of

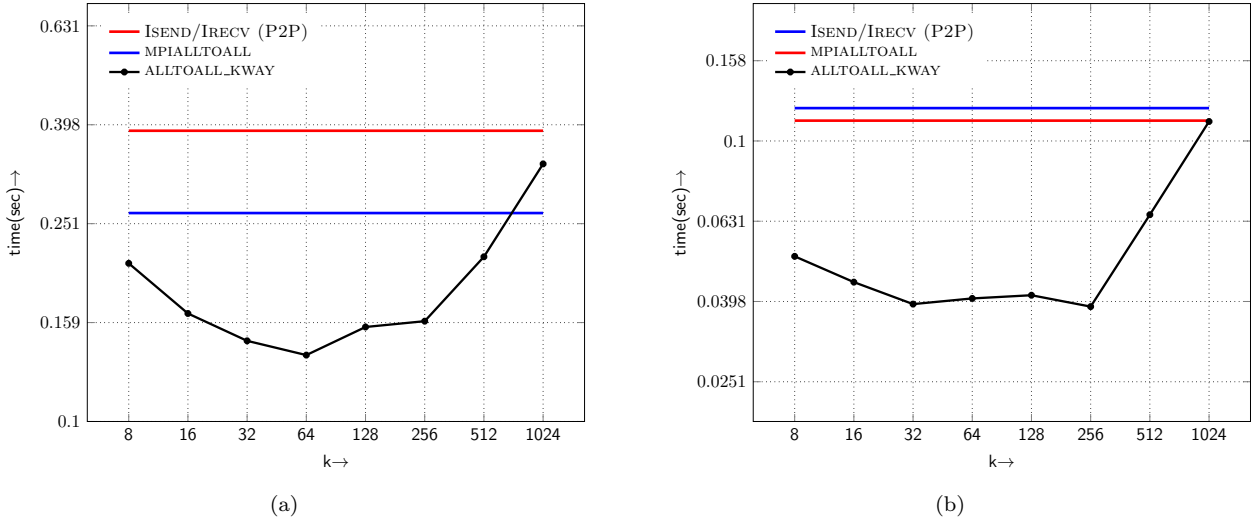


Figure 3: The timings are given for different splitting parameter, k in our kway all-to-all (denoted by ALLTOALL_KWAY). The optimal transpose time corresponds to $k = 64$. (a) Times for performing a transpose of size 2048^3 on 16384 cores of Stampede, Fig. 4. (b) Times for performing a transpose of size 2048^3 on cores of 512 GPUs on Titan.

length N_0 should be computed after this step. Now in the Fourier space, each task owns the x pencil locally, while in spatial domain it owns the z dimension locally. This can be changed by performing two more all-to-all exchanges, but it is typically avoided as it can be done while the inverse FFT is being computed. The pencil decomposition algorithm can be extended to support nD tensors as shown in Algorithm 3.

It is well known that the most expensive part of distributed FFT is the communication phase [8], which adversely affects the scaling at large core counts. This has been verified in large scale runs on Stampede and Blue waters [20]. This phase involves all-to-all exchanges, which is essentially transpose operation between a subgroup of tasks. As mentioned earlier, this exchange should be wrapped around a packing/unpacking phase to make the data contiguous in the memory. Generally the packing/unpacking phase accounts for less than 10% of the transpose time on CPU, and a negligible time on GPUs. This phase can be performed either by reshuffling of the data as done in P3DFFT, a local transpose as implemented in FFTW library, or eliminated by using MPI Data types

[33]. Even with these methods the communication time dominates the cost of distributed FFT. The situation is even worse for the GPU, since the data has to be transferred forth and back to the CPU through PCIe, which is as expensive as the communication phase. For this reason we have implemented specific all-to-all operations which can alleviate this bottleneck. The easiest to implement all-to-all exchange is a point-to-point communication scheme, where each task sends and receives data from all the other tasks. The all-to-all exchange finishes in p steps with a total of $\mathcal{O}(N)$ data transfer. This option is superior for small number of processes. Although, this implementation provides us with a working all-to-all that can be tuned for the exchange operation on CPU/GPU, its performance degrades considerably for large core counts. This is due to the network congestion that happens for large tasks which adversely affects the performance. Methods such as waiting after sending a few messages can alleviate this problem, but they cannot solve the poor scaling problem. A paradigm change can solve this problem by sending the data in multiple stages such as done in the Bruck algorithm [5], or a newer zero copy method [39].

The Bruck algorithm is one of the methods implemented in MPI_ALLTOALL. To be able to alter the code and tune it for our needs, we have to implement our own implementation. This is specially critical for hiding PCIe overhead in the GPU code. As a result, we have optimized a more general in house exchange method that uses a k -way recursive doubling algorithm [35]. This all-to-all exchange alleviates the overhead associated with sending messages to a large number of tasks. In this method each task first sends the data recursively to k other tasks, instead of 2 as in Bruck's algorithm. The pseudo-code for the algorithm is given in Algorithm 5. In this method one transfers $\mathcal{O}(N \log p / \log k)$ data in $\log k$ steps. An example of the kway all-to-all in shown in Fig. 2 for $P = 9$, and $k = 3$. One can see that the algorithm reduces to point-to-point scheme when $k = p$. Our library selects the best all-to-all algorithm during the planing phase (Fig. 3).

Algorithm 4: SENDRECV_KWAY

Input : $comm, p$ (assume $p = mk$) p_r of current task in $comm$, messages $\{M_i^j \mid i \in I_j\}$ destined for task $p_j, \forall j \in comm$, global number of processes P .
Output: new communicator $comm'$, $p' = m = p/k$, messages $\{R_i^j \mid i \in \hat{I}_j\}$ destined for task $p'_j \in comm' \ \forall j$.
 $R \leftarrow \emptyset$
 $color \leftarrow \lfloor k p_r / p \rfloor$
for $i \in 1, \dots, k - 1$ **do**
 $prev \leftarrow m((color - i) \bmod k) + (p_r \bmod m)$
 $R \leftarrow R \cup MPI_Irecv(prev, comm)$
for $i \in 1, \dots, k - 1$ **do**
 $prev \leftarrow m((color - i) \bmod k) + (p_r \bmod m)$
 $psend \leftarrow m((color + i) \bmod k) + (p_r \bmod m)$
 $MPI_Issend(M^s \mid m \leq s < m(i+1), psend, comm)$
 $MPI_WaitRecv(prev)$
 $MPI_WaitAll()$
 $comm' \leftarrow MPI_Comm_split(color, comm)$
return $[R, comm']$

An important advantage of these algorithms is hiding PCIe overhead between GPU and CPU, during the all-to-all exchange phase. Recently, NVIDIA has introduced GPUDirect technology where GPUs on different nodes can communicate directly through the PCIe bus and

Algorithm 5: ALLTOALLV_KWAY

Input : $comm, p$ (assume $p = k^l$), p_r of current task in $comm$, message $M_{p_r}^i$ destined for task $p_i \ \forall i$
Output: message $M_i^{p_r}$ received from task $p_i \ \forall i$
 $P = p$; $\text{iterations: } \mathcal{O}(\log p / \log k)$
do
 $[M, comm] \leftarrow \text{SendRecv_kway}(\{M_i^j\}, comm, P);$

avoid the CPU altogether. However, this feature requires special hardware support as well as a compatible OFED (OpenFabrics Enterprise Distribution). In the absence of GPUDirect, one option is to perform a blocking memcpy from GPU to CPU, use the transpose functions that are already implemented in the CPU code, and then copy back the results to the GPU. The packing and unpacking phases can still be performed on the GPU, as it can perform the reshuffling/local transposes much faster than CPU.

However, it is possible to hide the extra cost of memcpy by interleaving it into send and receive operations. This is specially easy in the point-to-point exchange. Instead of copying all the data at once and then sending it, we divide the memcpy into chunks of the same size that each process has to send to other tasks. Each chunk is copied to a CPU buffer at a time, followed by an asynchronous send instruction. In this manner, the communication part of the CPU can start while the rest of the chunks are being copied. Since we post the asynchronous receive instructions beforehand, the receive operation can also happen with the device to host memcpy. Each received chunk can then be copied asynchronously back to the GPU. A similar approach can be used in the k -way all-to-all scheme. In the first phase of the algorithm, we interleave device to CPU memcpy with send/recv operations. For the rest of the $\log k$ steps, except for the last one, only CPU memcpy will be used as the send/recv happens between CPU buffers. However, in the last step we again interleave memcpy from CPU to GPU, to efficiently hide the PCIe overhead.

Complexity analysis. The communication cost is $\mathcal{O}(\frac{N}{\sigma(p)})$, where $\sigma(p)$ is the bisection bandwidth of the network (for a hypercube it is $p/2$ [29]). The total execution time for an FFT of size N on a hypercube can be approximated by:

$$T_{\text{FFT}} = \mathcal{O}\left(\frac{N \log N}{P}\right) + \mathcal{O}\left(\frac{N}{P}\right).$$

The first term represents the computation and the second the memory and communication costs. For a 3-D torus topology (such as the one used on Titan) the complexity becomes:

$$T_{\text{FFT}} = \mathcal{O}\left(\frac{N \log N}{P}\right) + \mathcal{O}\left(\frac{N}{P^{2/3}}\right).$$

For the GPU version this should also include the device-host communication costs. In [8] the authors give a detailed analysis in which cache effects and the local and remote memory bandwidth for GPUs and CPUs is taken into account. The basic point is that in strong scaling, the computation part becomes negligible and the overall wall-clock time will be dominated by the communication costs.

3. Numerical experiments

In this section we report the performance of AccFFT and give details regarding our implementation and the different problem sizes used for evaluating the library.

Computing Platforms

The tests are performed on the following platforms:

- The **Stampede** system at TACC is a Linux cluster consisting of 6400 compute nodes, each with dual, eight-core processors for a total of 102,400 available CPU-cores. Each node has two eight-core 2.7GHz Intel Xeon E5 (Sandy Bridge) processors with 2GB/core of memory and a three-level cache. Stampede has a 56GB/s FDR Mellanox InfiniBand network connected in a fat tree configuration.
- The **Maverick** system at TACC is a Linux cluster with 132 compute nodes, each with dual 10-core

2.8GHz Intel Xeon E5 (Ivy Bridge) processors with 13GB/core of memory equipped with FDR Mellanox InfiniBand network.

- The **Titan** system is a Cray XK7 supercomputer at ORNL. Titan has a total of 18,688 nodes consisting of a single 16-core AMD Opteron 6200 series processor, for a total of 299,008 cores. Each node has 32GB of memory. It is also equipped with a Gemini interconnect and 600 terabytes of memory across all nodes. In addition, all of Titan's 18,688 compute nodes contain an NVIDIA Tesla K20 graphics processing unit.

Implementation Details. All algorithms described in this work were implemented using C++, OpenMP and MPI. The only external libraries used were the MPI, FFTW, and CUFFT. On Titan, we used the GCC compiler and the CRAY-MPICH libraries. On Stampede and Maverick we used the Intel compilers and the Intel MPI library. We compare our CPU code with P3DFFT (version 2.7.2) and PFFT (version 1.0.8 alpha) libraries, and the GPU code with FFTE library (version 6.0). The GPU code for FFTE library is written in Fortran and requires the commercial PGI compiler, and cuFFT for its FFT computations on the GPU. All the libraries were compiled with the MEASURE planner flag where applicable. This flag is used to tune the libraries to the machine used. Special attention was paid to use the best configuration for each library to perform a fair comparison. All the timings are the average of 10-100 repetition of the kernels. The timings for the first two runs for all libraries is discarded for warm up. All results were computed in double precision.

Parameters in the Experiments The parameters in our runs are the problem size N_0, N_1, N_2 , the number of tasks P , the type of all-to-all primitive used in the transpose (chosen automatically by direct evaluation), and the use of CPU or GPU. In most of the tests, we use $N_0 = N_1 = N_2$. The exception is two tests in which we test the library with non well-structured matrices, and a 4D test case. In

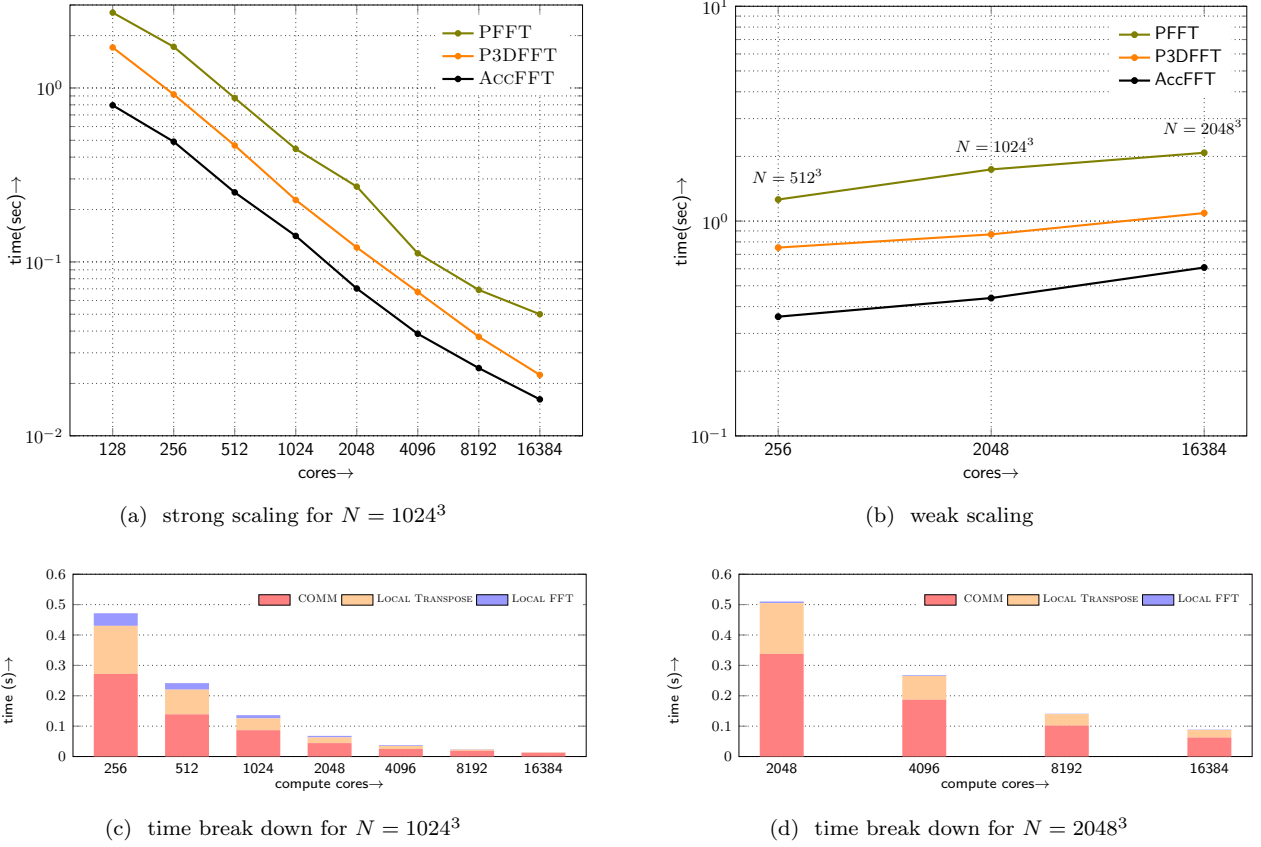


Figure 4: CPU scaling results of AccFFT on Stampede. Wall-clock time is given for different core counts for a forward R2C FFT.

all our runs, we use one MPI task per NUMA socket. In all platforms this corresponds to two MPI tasks per node. We use R2C to denote real-to-complex FFTs and C2C to denote complex to complex. Roughly speaking, the C2C transform has double the computation and communication compared to R2C transform. All timings are in seconds.

Experiments First we examine the performance of our code on the TACC systems, and then we discuss the results on Titan.

- In the first experiment (Fig. 4 a) we study the strong scaling of AccFFT for a problem size of 1024^3 from 128 to 16,384 cores corresponding to 8 and 1024 nodes of Stampede, respectively. Overall the CPU code achieves a good scalability. The parallel efficiency from 512 to 16K cores is approximately 48%, indicating that we could push the core count further and still get good speedup. One can observe that AccFFT is roughly 2-3 times faster than P3DFFT and

PFFT. A similar trend is observed in the weak scaling test shown in Fig. 4(b).

The breakdown of the timings for $N = 1024^3$ and $N = 2048^3$ is given in Fig. 4 (c-d). It is observed that the communication phase is the most expensive part, while the local FFT computation has negligible cost.

- The above experiment is repeated with a non well-structured size of $N = 256 \times 512 \times 1024$ on Maverick using both the CPU and the GPU code (Fig. 5 (a)). As one can see, our GPU code reaches the same performance as the CPU code, which is due to the effective coalescing of all-to-all operation with CPU-GPU and GPU-CPU memcpy. Weak scaling analysis shows the same trend, as shown in Fig. 5 (b).

There is currently no open source GPU code that supports pencil decomposition, other than digpufft and FFTE. The digpufft library, which is built on top of

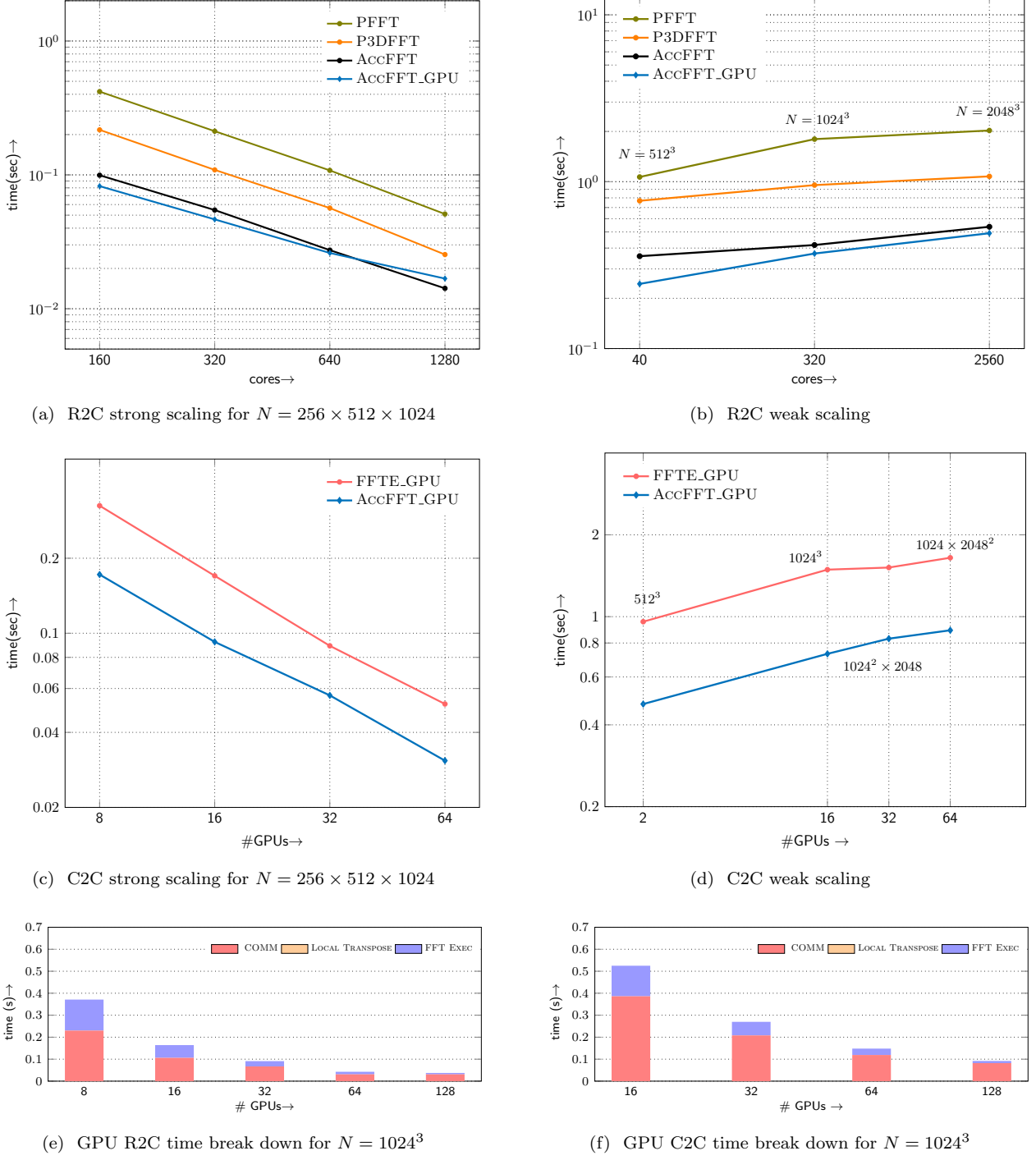


Figure 5: Scaling results of AccFFT performed on Maverick. CPU comparison is only made for R2C, as P3DFFT does not support C2C transforms. (a) strong scaling result for a non-structured R2C transform of size $N = 256 \times 512 \times 1024$, (b) R2C weak scaling, (c) C2C Strong scaling for $N = 256 \times 512 \times 1024$ and comparison with FFTE's GPU code, (d) C2C weak scaling, (e) breakdown of timings for R2C transform of size $N = 1024^3$, (f) breakdown of timings for C2C transform of size $N = 1024^3$.

| # Cores | Total | Comm | FFT | (Un)Pack | # GPUs | Total | Comm | FFT | (Un)Pack |
|---------|-------|-------|--------|----------|--------|-------|-------|---------|----------|
| 2048 | 0.144 | 0.092 | 0.0116 | 0.0383 | 128 | 0.138 | 0.131 | 0.00097 | 0.0052 |
| 4096 | 0.121 | 0.095 | 0.0058 | 0.0196 | 256 | 0.078 | 0.073 | 0.00054 | 0.0046 |
| 8192 | 0.057 | 0.044 | 0.0029 | 0.0093 | 512 | 0.050 | 0.046 | 0.00027 | 0.0025 |
| 16K | 0.039 | 0.032 | 0.0015 | 0.0051 | 1024 | 0.032 | 0.028 | 0.00020 | 0.0025 |
| 32K | 0.022 | 0.019 | 0.0007 | 0.0022 | 2048 | 0.027 | 0.025 | 0.00020 | 0.0014 |
| 65K | 0.016 | 0.012 | 0.0004 | 0.0014 | 4096 | 0.016 | 0.014 | 0.00016 | 0.0018 |

Table 1: *Strong scaling results for AccFFT performed on Titan. Timings are given for R2C transform of size $N = 1024^3$ on CPU and GPU (left/right). The breakdown of the total time in terms of local FFT computations, packing and unpacking (local transpose), and the communication times is given for different core counts. Note that there is one GPU per node on Titan, and so the 128 GPU test should be compared with the 2048-core CPU run.*

| # Cores | Total | Comm | FFT | (Un)Pack |
|---------|-------|--------|--------|----------|
| 2048 | 2.00 | 1.12 | 0.57 | 0.285 |
| 4096 | 1.14 | 0.846 | 0.151 | 0.142 |
| 8192 | 0.898 | 0.735 | 0.0798 | 0.077 |
| 16K | 0.375 | 0.297 | 0.0377 | 0.037 |
| 32K | 0.368 | 0.297 | 0.0376 | 0.014 |
| 65K | 0.232 | 0.198 | 0.0202 | 0.009 |
| 131K | 0.116 | 0.0974 | 0.0115 | 0.004 |

Table 2: *Strong scaling results for AccFFT performed on Titan. Total time is given for CPU R2C forward FFT of size $N = 2048^3$. The breakdown of the total time in terms of local FFT computations, packing and unpacking (local transpose), and the communication time are given.*

P3DFFT, is no longer maintained and our attempts to run it were not successful. However, FFTE library is maintained and supports C2C transforms with pencil decomposition [36]. Both our library as well as FFTE use cuFFT for local FFT computations. The two libraries are compared in Fig. 5 (c-d). AccFFT is consistently $2\times$ faster in both the strong and weak scaling tests.

The break down of the timings for R2C and C2C transforms for $N = 1024^3$ is shown in figures 5 (e-f). An interesting observation is that the local data shuffling has a negligible time on GPU, and the communication phase dominates the cost.

- Now we switch to Titan, where we consider the strong scaling of the CPU and GPU versions of our code. The

results are given in Tables 1 and 2 for up to 4096 GPUs and 131K cores (Notice that there is 1GPU per node and 16 cores per node on Titan). The efficiency for the largest CPU run is 27% for a $64\times$ increase in the core count. The GPU code achieves the same efficiency for a $32\times$ increase in the number of GPUs. Again, we do not use any GPUDirect feature on Titan, but still, the GPU timings are either better or the same as that of the CPU. This is evident by looking at the `comm` time for both CPU and GPU. The GPU’s communication time consists of the time for mem-cpy forth and back from the CPU as well as the all-to-all communication. Another interesting point is that the local FFT computation is almost an order of magnitude faster on GPU compared to the CPU.

- Finally, as a proof of concept we show how the code can be used for high dimensional transforms. In certain applications such as in signal processing, one needs to compute FFT of a 4D array, where the last dimension corresponds to time. Table 3 shows the strong scaling of the CPU code for a C2C transform of size $N = 512 \times 256 \times 128 \times 64$. Nothing changes in our communication algorithms for high dimensional transforms for either the CPU or the GPU code.

| # Cores | Total | Comm | FFT | (Un)Pack |
|---------|--------|-------|--------|----------|
| 512 | 0.427 | 0.254 | 0.0369 | 0.130 |
| 1024 | 0.242 | 0.151 | 0.0204 | 0.065 |
| 2048 | 0.141 | 0.094 | 0.0099 | 0.033 |
| 4096 | 0.0797 | 0.053 | 0.0044 | 0.017 |
| 8192 | 0.0536 | 0.034 | 0.0018 | 0.008 |
| 16384 | 0.0423 | 0.029 | 0.0010 | 0.004 |

Table 3: *CPU strong scaling results of AccFFT using the pencil decomposition algorithm for a four dimensional problem size of $512 \times 256 \times 128 \times 64$ on Stampede. Wall-clock time is given for different core counts for a forward C2C FFT.*

4. Conclusions

We presented AccFFT, a library for distributed memory FFTs with several unique features: distributed GPU calculations, multiple all-to-all variants for performance tuning, communication overlap using pipelining for the GPU version, and support for real and complex transforms.

The performance of the library was tested on three different machines: The Stampede and Maverick systems at TACC, as well as the Titan system at ORNL. The largest test corresponds to 131K cores as well as 4,096 GPUs of Titan. This is the largest FFT that has been scaled on GPUs. The CPU performance tests show a consistent $2 - 3 \times$ speedup over P3DFFT and PFFT libraries. A similar speedup of $2 \times$ is observed for the GPU code when compared to FFTE library. To the best of our knowledge, the latter is the only open source library supporting pencil decomposition for GPUs.

This work is by no means complete with these results. We are currently working on coupling the tuning process with the theoretical model developed in [8]. Using non-blocking collectives can further accelerate the calculations, if the user interleave other computations while the FFT communication is completing. Other possibilities include distributing the data to both the CPU and GPU on each node. This has been shown to be an effective strategy on single node computations [41]. Another possibility is to

extend the method to Xeon Phi accelerators, which we are currently working on.

Acknowledgment

We would like to thank Robert van de Geijn, Jesper Larsson Traff, and Martin Schatz for useful discussion on optimizing all-to-all. We would like to thank Bill Barth, Carlos Rosales, and John McCalpin for helping us with the code as well as providing valuable insight. Computing time on the Texas Advanced Computing Centers Stampede system was provided by an allocation from TACC and the NSF.

References

- [1] <https://github.com/clMathLibraries/clFFT>.
- [2] <https://github.com/amirgholami/accfft>.
- [3] S. AARSETH, *Gravitational N-body simulations*, Cambridge Univ Pr, 2003.
- [4] O. AYALA AND L.-P. WANG, *Parallel implementation and scalability analysis of 3-D Fast Fourier Transform using 2d domain decomposition*, Parallel Computing, 39 (2013), pp. 58–77.
- [5] J. BRUCK, C.-T. HO, S. KIPNIS, E. UPFAL, AND D. WEATHERSBY, *Efficient algorithms for all-to-all communications in multiport message-passing systems*, Parallel and Distributed Systems, IEEE Transactions on, 8 (1997), pp. 1143–1156.
- [6] O. P. BRUNO AND L. A. KUNYANSKY, *A fast, high-order algorithm for the solution of surface scattering problems: Basic implementation, tests, and applications*, Journal of Computational Physics, 169 (2001), pp. 80–110.
- [7] A. BUENO-OROVIO, V. M. PÉREZ-GARCÍA, AND F. H. FENTON, *Spectral methods for partial differential equations in irregular domains: the spectral smoothed boundary method*, SIAM Journal on Scientific Computing, 28 (2006), pp. 886–900.
- [8] K. CZECHOWSKI, C. BATTAGLINO, C. MCCLANAHAN, K. IYER, P.-K. YEUNG, AND R. VUDUC, *On the communication complexity of 3-D FFTs and its implications for exascale*, in Proceedings of the 26th ACM International Conference on Supercomputing, ICS ’12, New York, NY, USA, 2012, ACM, pp. 205–214.
- [9] R. O. DROR, J. GROSSMAN, K. M. MACKENZIE, B. TOWLES, E. CHOW, J. K. SALMON, C. YOUNG, J. A. BANK, B. BATSON, M. M. DENEROFF, J. S. KUSKIN, R. H. LARSON, M. A. MORAES, AND D. E. SHAW, *Exploiting 162-Nanosecond End-to-End Communication Latency on Anton*, in 2010 ACM/IEEE Interna-

tional Conference for High Performance Computing, Networking, Storage and Analysis, IEEE, Nov. 2010, pp. 1–12.

[10] T. V. T. DUY AND T. OZAKI, *A decomposition method with minimum communication amount for parallelization of multi-dimensional FFTs*, Computer Physics Communications, 185 (2014), pp. 153 – 164.

[11] S. FILIPPONE, *The IBM parallel engineering and scientific subroutine library*, in Applied Parallel Computing Computations in Physics, Chemistry and Engineering Science, Springer, 1996, pp. 199–206.

[12] F. FRANCHETTI, Y. VORONENKO, AND G. ALMASI, *Automatic generation of the HPC challenge global FFT benchmark for Blue Gene/P*, in High Performance Computing for Computational Science-VECPAR 2012, Springer, 2013, pp. 187–200.

[13] M. FRIGO AND S. G. JOHNSON, *FFTW home page*. <http://www.fftw.org>.

[14] M. FRIGO AND S. G. JOHNSON, *The design and implementation of FFTW3*, Proceedings of the IEEE, 93 (2005), pp. 216–231.

[15] H. GAHVARI AND W. GROPP, *An introductory exascale feasibility study for FFTs and multigrid*, in 2010 IEEE International Symposium on Parallel & Distributed Processing (IPDPS), IEEE, 2010, pp. 1–9.

[16] A. GRAMA, A. GUPTA, G. KARYPIS, AND V. KUMAR, *An Introduction to Parallel Computing: Design and Analysis of Algorithms*, Addison Wesley, second ed., 2003.

[17] L. GU, J. SIEGEL, AND X. LI, *Using GPUs to compute large out-of-card FFTs*, in Proceedings of the international conference on Supercomputing, ACM, 2011, pp. 255–264.

[18] K. KANDALLA, H. SUBRAMONI, K. TOMKO, D. PEKUROVSKY, S. SUR, AND D. K. PANDA, *High-performance and scalable non-blocking all-to-all with collective offload on infiniband clusters: a study with parallel 3-D FFT*, Computer Science-Research and Development, 26 (2011), pp. 237–246.

[19] D. KOZAKOV, R. BRENKE, S. R. COMEAU, AND S. VAJDA, *Piper: An FFT-based protein docking program with pairwise potentials*, Proteins: Structure, Function, and Bioinformatics, 65 (2006), pp. 392–406.

[20] M. LEE, N. MALAYA, AND R. D. MOSER, *Petascale direct numerical simulation of turbulent channel flow on up to 786k cores*, in Proceedings of SC13: International Conference for High Performance Computing, Networking, Storage and Analysis, ACM, 2013, p. 61.

[21] N. LI AND S. LAIZET, *2DECOMP & FFT-a highly scalable 2d decomposition library and FFT interface*, in Cray User Group 2010 conference, 2010, pp. 1–13.

[22] D. M. MCQUEEN AND C. S. PESKIN, *Shared-memory parallel vector implementation of the immersed boundary method for the computation of blood flow in the beating mammalian heart*, Journal Of Supercomputing, 11 (1997), pp. 213–236.

[23] J. C. MICHEL, H. MOULINÉC, AND P. SUQUET, *Effective properties of composite materials with periodic microstructure: a computational approach*, Comput. Methods Appl. Mech. Engrg, 172 (1999).

[24] N. NANDAPALAN, J. JAROS, A. P. RENDELL, AND B. TREEBY, *Implementation of 3-D FFTs across multiple GPUs in shared memory environments*, in Parallel and Distributed Computing, Applications and Technologies (PDCAT), 2012 13th International Conference on, IEEE, 2012, pp. 167–172.

[25] A. NUKADA, K. SATO, AND S. MATSUOKA, *Scalable multi-GPU 3-D FFT for TSUBAME 2.0 supercomputer*, in High Performance Computing, Networking, Storage and Analysis (SC), 2012 International Conference for, IEEE, 2012, pp. 1–10.

[26] C. NVIDIA, *CUFFT library*, 2010.

[27] D. OROZCO, E. GARCIA, R. PAVEL, O. AYALA, L.-P. WANG, AND G. GAO, *Demystifying performance predictions of distributed FFT 3-D implementations*, in Network and Parallel Computing, Springer, 2012, pp. 196–207.

[28] J. PARK, G. BIKSHANDI, K. VAIDYANATHAN, P. T. P. TANG, P. DUBEY, AND D. KIM, *Tera-scale 1d FFT with low-communication algorithm and Intel® Xeon Phi coprocessors*, in Proceedings of SC13: International Conference for High Performance Computing, Networking, Storage and Analysis, ACM, 2013, p. 34.

[29] D. PEKUROVSKY, *P3DFFT: A framework for parallel computations of Fourier transforms in three dimensions*, SIAM Journal on Scientific Computing, 34 (2012), pp. C192–C209.

[30] J. PHILLIPS AND J. WHITE, *A precorrected-FFT method for electrostatic analysis of complicated 3-d structures*, Computer-Aided Design of Integrated Circuits and Systems, IEEE Transactions on, 16 (1997), pp. 1059–1072.

[31] M. PIPPIG, *PFFFT: An extension of FFTW to massively parallel architectures*, SIAM Journal on Scientific Computing, 35 (2013), pp. C213–C236.

[32] M. PIPPIG AND D. POTTS, *Parallel three-dimensional nonequispaced Fast Fourier Transforms and their application to particle simulation*, SIAM Journal on Scientific Computing, 35 (2013), pp. C411–C437.

[33] M. SCHATZ, J. POULSON, AND R. A. VAN DE GEIJN, *Parallel matrix multiplication: A systematic journey.*, (submitted to) SIAM Journal on Scientific Computing, (2014).

[34] S. SONG AND J. K. HOLLINGSWORTH, *Scaling parallel 3-D FFT with non-blocking MPI collectives*, in Proceedings of the 5th Workshop on Latest Advances in Scalable Algorithms for Large-Scale Systems, ScalA '14, Piscataway, NJ, USA, 2014, IEEE Press, pp. 1–8.

[35] H. SUNDAR, D. MALHOTRA, AND G. BIROS, *HykSort: A new*

variant of hypercube quicksort on distributed memory architectures, in ICS'13: Proceedings of the International Conference on Supercomputing, 2013, 2013.

[36] D. TAKAHASHI, *An implementation of parallel 3-D FFT with 2-d decomposition on a massively parallel cluster of multi-core processors*, in Parallel Processing and Applied Mathematics, Springer, 2010, pp. 606–614.

[37] D. TAKAHASHI, *Implementation of parallel 1-d FFT on GPU clusters*, in Computational Science and Engineering (CSE), 2013 IEEE 16th International Conference on, Dec 2013, pp. 174–180.

[38] P. T. P. TANG, J. PARK, D. KIM, AND V. PETROV, *A framework for low-communication 1-D FFT*, Scientific Programming, 21 (2013), pp. 181–195.

[39] J. L. TRÄFF, A. ROUGIER, AND S. HUNOLD, *Implementing a classic: zero-copy all-to-all communication with MPI datatypes*, in Proceedings of the 28th ACM international conference on Supercomputing, ACM, 2014, pp. 135–144.

[40] E. WANG, Q. ZHANG, B. SHEN, G. ZHANG, X. LU, Q. WU, AND Y. WANG, *Intel math kernel library*, in High-Performance Computing on the Intel® Xeon Phi, Springer, 2014, pp. 167–188.

[41] J. WU AND J. JAJA, *Optimized strategies for mapping three-dimensional FFTs onto CUDA GPUs*, in Innovative Parallel Computing (InPar), 2012, IEEE, 2012, pp. 1–12.